Ecological Informatics 90 (2025) 103293

Contents lists available at ScienceDirect

Ecological Informatics

journal homepage: www.elsevier.com/locate/ecolinf

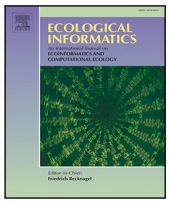

Intratentacular budding and zooid-dynamics in two coral genera

Matan Yuval [a,b,c,*], Amit Peleg [a], Elvan Ceyhan [d], Dan Tchernov [b], Yossi Loya [e], Avi Bar-Massada [f], Tali Treibitz [a]

[a] School of Marine Sciences, University of Haifa, Haifa 3498838, Israel
[b] The Interuniversity Institute for Marine Sciences of Eilat, Eilat 8810302, Israel
[c] Charles Darwin Research Station, Charles Darwin Foundation, Santa Cruz, Galápagos, 200102, Ecuador
[d] Department of Mathematics and Statistics, Auburn University, Auburn, AL 36849, USA
[e] School of Zoology, Tel-Aviv University, Tel Aviv 6997801, Israel
[f] Department of Biology and Environment, University of Haifa at Oranim, Kiryat Tivon 36006, Israel

ARTICLE INFO

Dataset link: https://doi.org/10.5281/zenodo.14783315, https://github.com/MatanYuval/ReefMetrics/tree/main/ZooidSeg, https://github.com/VISEAON-Lab/mal-coral

Keywords:
Coral reefs
Zooids
Cyclical morphogenesis
Intratentacular budding
3D Instance segmentation
Underwater photogrammetry

ABSTRACT

Zooids are the basic modules of colonial organisms. Despite the fact that they are the building blocks of coral colonies and by extension, of coral reefs, the role that zooids play in determining coral colony structure and growth has remained severely overlooked in ecological research. The patterns of addition of zooids (budding mechanics) determine much of the colony's shape and function. Yet because zooids are small in size and large in numbers, ecological studies often focus on coral colonies as unitary organisms and little is known about how zooids vary within and between colonies and species. Nevertheless, advances in computer vision and deep learning create an opportunity to count and classify zooids on the reef scale and to infer their role in colony growth and structure.

Here we present the first quantitative analysis of zooid morphogenesis in two coral genera captured in situ. These genera, *Lobophyllia* and *Dipsastraea*, represent two evolutionarily distinct forms of corals. We classified over 6000 zooids according to their developmental phase to study their basic attributes including size, association with structural complexity, and intra-colony neighbor relations. Our findings suggest that the morphogenetic cycle of zooids is conserved and size-dependent, that budding mechanics are associated with structural complexity, and that zooids form coalitions by developmental phase implying concentrated growth and stagnation.

The zooid-centric approach is transferable and scalable and can be implemented to track corals in different applications from nurseries to wide scale monitoring programs. It can improve our understanding of coral colony formation, and how coral colonies and individual zooids react to disturbances such as physical damage from storms, coral bleaching, and pollution.

This work bridges the gap between theory and in situ observations, making it a valuable resource for informing other research on coral colony formation and growth modeling, self-organization in modular systems, and coral reef restoration strategies. Moreover, our dataset has broad interdisciplinary value, with potential applications ranging from computer graphics and geometric modeling to studies of natural tiling patterns and spatial organization in biological systems.

1. Introduction

It has long been argued that morphological hierarchy (i.e., nesting and modularity) persists across organizational levels and phyla and therefore is an absolute phenomenon (D'Arcy, 1942; Riedl, 1978). Modularity is the repetition of sub-units. Defining its role for a given entity such as a colonial organism has far-reaching implications in developmental biology, ecology, and evolution (Hiebert et al., 2021; Tuomi and Vuorisalo, 1989) as it allows broad conclusions to be drawn about information packing in complex systems and the ability to produce complex phenomena from a simple set of rules (Wolfram, 1984).

Corals are modular, colonial organisms (Medellín-Maldonado et al., 2022; Rosen, 1986). They are composed of modular units that can be divided in smaller complete and equivalent (homogeneous) units until the sequence is broken by non-equivalent (heterogeneous) units.

This study focuses on coral zooids, the basic first order module (cannot be divided into smaller homogeneous units) of coral colonies (Kaandorp et al., 2005; Merks et al., 2004; Re et al., 2024).

* Corresponding author at: School of Marine Sciences, University of Haifa, Haifa 3498838, Israel.
E-mail address: mtnyvl@gmail.com (M. Yuval).

https://doi.org/10.1016/j.ecoinf.2025.103293
Received 7 September 2024; Received in revised form 12 May 2025; Accepted 20 June 2025
Available online 1 July 2025

Coral zooids were defined by Rosen (1986) as polyps[1] with their skeletal counterpart. Fig. 2, B highlights the difference between the zooid, polyp, and mouth. The skeleton deposited from the calice constitutes corallite, and a zooid is a polyp with the calice and corallite. In this work we follow Rosen's convention that "it is the combined corallite length and arrangement in a colony that gives a colony its particular form....and in the absence of a suitable term for a polyp with its corallite, and because of its fundamental importance as a unit of colony growth and form, we refer to the two together as zooids" (Rosen, 1986).

Modularity facilitates the phenotypic plasticity of the colonial form (Rosen, 1986) by enabling zooids to come together in different configurations to manifest a variety of shapes (Mackie, 1986). Moreover, coral zooids are the basic modules of a hierarchical ecosystem: coral reefs, deeming them a critical organizational level (O'Neill, 1986). Therefore, a zooid-centric approach to coral ecology — focusing on corals as colonial organisms rather than unitary organisms (Dornelas et al., 2017; Re et al., 2024; Rosen, 1986) can help parse apart the role of zooids in coral colony formation and, by extension, the ecosystem services governed by these factors; these include, but are not limited to, ecosystem engineering, coastal protection, fisheries support, biodiversity maintenance, and carbon sequestration (Jones et al., 1994; Woodhead et al., 2019).

A zooid can be defined by a skeletal segment — the calice, and multiplies (also) by budding: a form of asexual reproduction (cloning), via two main mechanisms: intra-tentacular budding (occurring within polyps) and extra-tentacular budding (occurring between polyps, Fig. 1, B). It was suggested that intra-tentacular budding leads to similar functional capacity with regards to fecundity among zooids while extra-tentacular budding lead to higher colony integration and a range of zooid sizes in the colony (Soong and Lang, 1992). Another study suggested that a conserved threshold of the perimeter over diameter of zooids controls intratentacular budding and underestimated budding to take an average of 12 months (Gateno and Rinkevich, 2003). In another study, coral budding rates were found to vary seasonally (Lartaud et al., 2014). Another study showed that polyps tended to bud when there was open space near them (Sakai, 1998) and that the reproductive integration of zooids in a colony may be determined by the age and size of the colony (Kai and Sakai, 2008). Furthermore, the size and age of the colonies affect their reproduction capacity (Rapuano et al., 2023), and zooids of larger colonies tend to be more reproductive (Sakai, 1998). Recently, computed tomography was used to model trajectories of corallites and it was found that budding rates vary significantly according to the position they occupy within the colony (Medellín-Maldonado et al., 2022). Merks et al. (2004) modeled branching laws in coral growth using a zooid centric approach and found that the shape of the zooid is important for the shape of the colony. A polyp-oriented model was also used to model coral colonies and it was found that this approach yields results non-distinguishable from 3D images of real colonies (Kaandorp et al., 2005). Yet, these approaches are limited in that they are not observed in situ, and rely either on model data or inferences from dead or fossil coral zooids.

In intratentacular budding, clonoteny is when zooids remain in contact and clonopary is when they become fully detached (Fig. 3, A). The continuum between clonoteny and clonopary constitutes the morphogenetic cycle (Fig. 3): zooids add mouths (clonoteny) and divide (clonopary) and can be classified based on the number of mouths as di-stomodeal, tri-stomodeal, and even polystomodeal (Matthai, 1926). Furthermore, several budding events (addition of mouths and skeletal divisions) can occur concurrently and discontinuously in a single zooid, resulting in a polystomodeal zooid with irregular outlines referred to here as an undecided form due to its plastic outline. Such zooids are capable of producing flexible tessellation (tiling of a 3D surface) patterns and are highly competitive and possibly adaptive (see Fig. 2, D for examples of the competitive advantages of the undecided form).

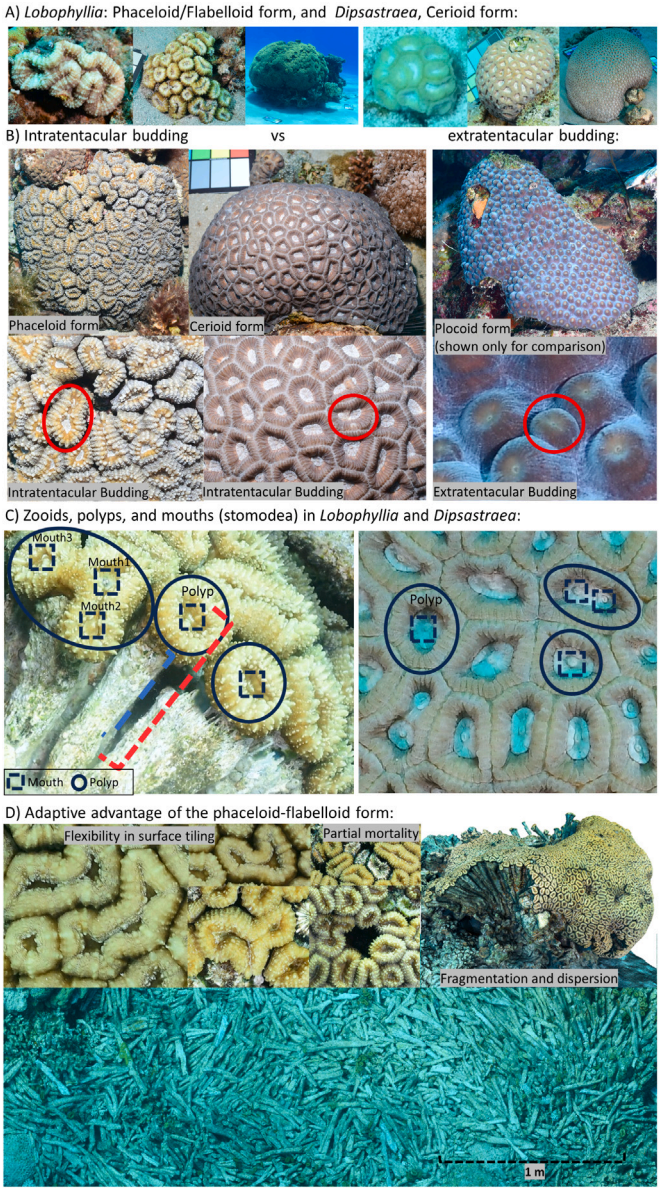

Fig. 1. Overview of colony and zooid structure and budding modes in *Lobophyllia* and *Dipsastraea* corals. (A) Colony morphologies of *Lobophyllia* showing the phaceloid/flabelloid form and *Dipsastraea* exhibiting the cerioid form. (B) Comparison of budding modes: Intratentacular budding where zooids are added within skeletal segment in phaceloid and cerioid forms (left and middle) versus extratentacular budding where zooids are added between segments in the plocoid form (right). Red circles highlight budding regions. It is important to note that this study does not address extratentacular budding and the example is just for comparison. (C) Organization of zooids, polyps, and mouths (stomodea) in *Lobophyllia* and *Dipsastraea*. Blue dashed boxes indicate individual mouths, and solid ovals outline polyps. The zooid is the polyp with its skeletal counterpart and is more pronounced in the phaceloid form. The undecided form in *Lobophyllia* is created by differential budding (e.g., three mouths on a single zooid), enabling more flexible tiling patterns. (D) The competitive advantages of the phaceloid-flabelloid form include flexible surface tiling especially by employing the undecided form. The right picture shows massive fragmentation of *Lobophyllia* zooids breaking under their own weight, the bottom picture shows massive dispersion following a storm (with 1 m scale bar).

In this study we focus on two coral genera: *Lobophyllia* and *Dipsastraea*, *Lobophyllia* belongs to the family Lobophyllidae (some fossils in the family date back to the Late Jurassic Geyer, 1954), and *Dipsastraea* belongs to the family Merulinidae that originated in the Oligocene (Jia

[1] Matthai (1926) defined polyps as "Any division of the soft parts of a colony which has a distinct circumoral tentacular boundary".

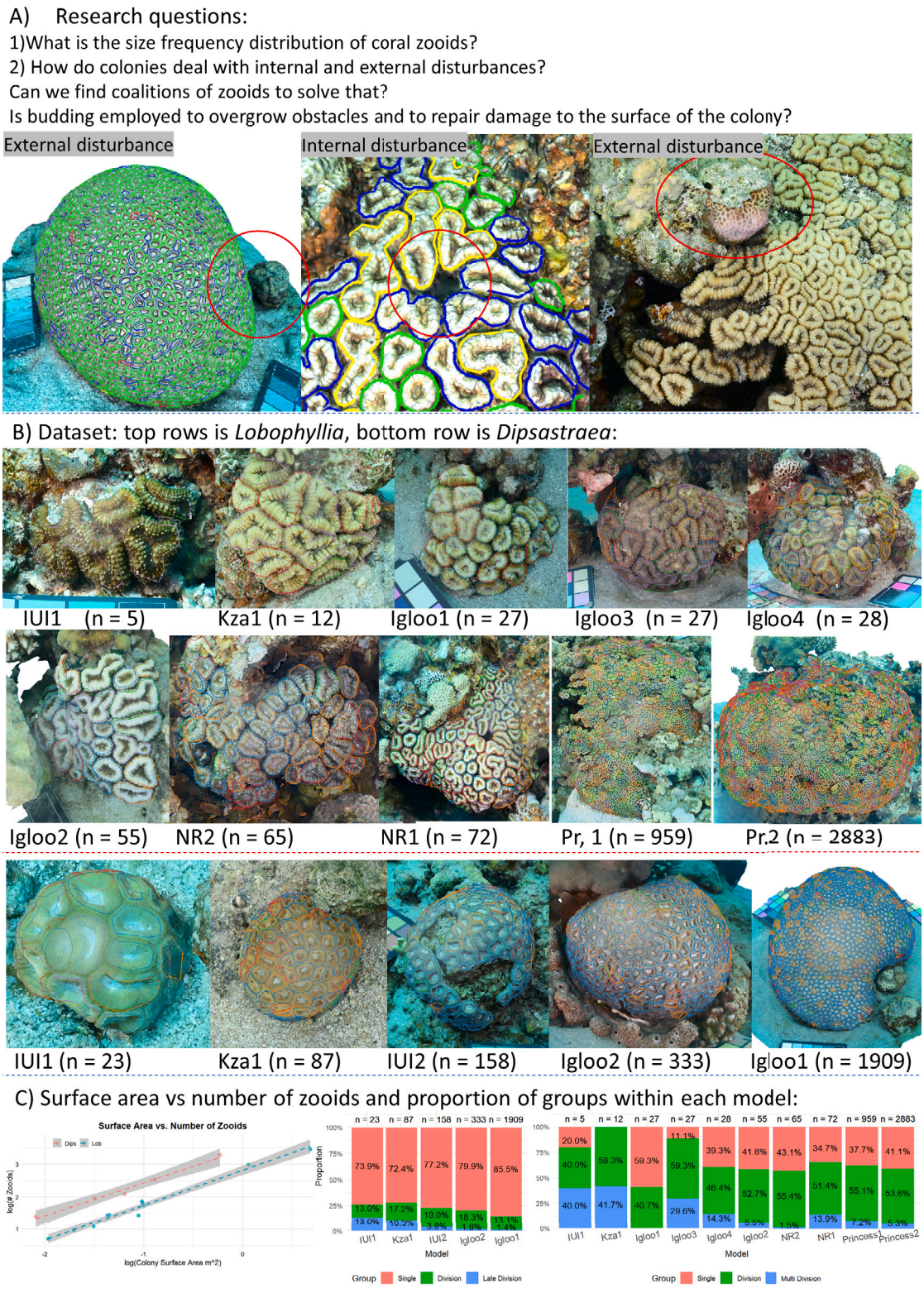

Fig. 2. Overview of research questions and dataset: (A) Research questions addressing the size frequency distribution of coral zooids and how colonies respond to internal and external disturbances, including the role of budding in surface tiling and obstacle avoidance. Examples of external (left and right images) and internal (middle image) disturbances are highlighted. The colors of the segments indicate their developmental phase. (B) Dataset images of *Lobophyllia* (top rows) and *Dipsastraea* (bottom row) colonies, with annotated zooids and sample sizes (n) provided for each colony. (C) Relationship between colony surface area and the number of zooids, showing a positive correlation for both *Dipsastraea* (n = 5, R^2 = 0.9836) and *Lobophyllia* (n = 10, R^2 = 0.9785) on a log–log scale. Bar plots illustrate the proportion of zooid groups within each colony, categorized into Single, Division, Late-Division, and Multi-Division groups.

et al., 2025). Both genera undergo intratentacular budding, but display two distinct colony forms (phaceloid, cerioid), representing primitive to evolved traits (Scrutton, 1998).

Zooids in phaceloid corals (e.g., *Lobophyllia*) are laterally free with supporting basal structures (Oliver, 1968, Fig. 1). This growth resembles the simplest form of cycle between clonopary and clonoteny. It is regarded the most primitive form of a coral colony (Rosen, 1986) and sometimes even referred to as a pseudo colony (Coates and Jackson, 1987; Stolarski et al., 2011) because its zooids are separated in the skeleton (Fedorowski, 1980; Scrutton, 1998).

In cerioid corals (e.g., *Dipsastraea*), the corallite is embedded in the colony and the zooids are grouped such that neighbors are in contact at all sides and each zooid is defined by a skeletal wall (Oliver, 1968). The complex phaceloid to flabello-meandroid[2] growth seen in *Lobophyllia* (Veron, 1986) probably involves multiple budding events with developmental offsets within a single zooid (Foster et al., 1988). On top of that, the cerioid form appears at an early stage in the phaceloid cycle and is thus considered paedomorphic (Poty, 2010, retaining the juvenile form in the adult, Fig. 3). This highlights heterochrony[3] in the budding process as a mechanism for the evolution of flabelloid and cerioid corals from a phaceloid ancestor (Pandolfi, 1988; Rosen, 1986).

We collected high-resolution 3D models of coral colonies from the Red Sea and identified three main types of zooids: Single (round/ hexagonal shape with one mouth), Division, (elongated/ figure-eight shapes, two mouths), in *Lobophyllia* we classified zooids which have irregular shapes and more than two mouths as Multi-Division and in *Dipsastraea* we classified zooids that have a skeletal wall forming in their middle as Late-Division (see Section 4.3). We refer to these classes as type/class throughout the manuscript.

We aimed to examine multiple questions related to zooid dynamics in *Lobophyllia* and *Dipsastraea* corals (Fig. 2, A): (1) If the size of coral zooids associated with their developmental phase (Fig. 3, Section 2.4), (2) if budding is associated with structural complexity (Fig. 4, Section 2.6), and (3) if zooids form non-random coalitions[4] within colonies (Fig. 5, Section 2.7).

To answer these questions, we developed state-of-the-art methods: To segment zooids, we used 3D instance segmentation[5] via Model Assisted Labeling (MAL[6]). For measuring the structural complexity around each zooid, we used plane-fitting (Fig. 4). To calculate zooid coalitions,[7] we used a K Nearest Neighbor Contingency Table (KNNCT, Fig. 5, Ceyhan, 2009; Dixon, 1994). Taken together, this enabled us to study 6,644 coral zooids across 15 coral colonies in both primitive and evolved coral genera (Scrutton, 1998, Fig. 2).

Crucially, although several studies have examined zooid dynamics and budding mechanics using 3D modeling technologies on the colony scale including micro-CT and optical tomography (e.g., Johanson et al., 2017; Li et al., 2020, 2023; Medellín-Maldonado et al., 2022), these were done on coral skeletons and not in situ. This is the first study to examine thousands of zooids across several coral colonies in a non-intrusive manner, offering a unique perspective on zooid dynamics under natural conditions.

2. Results

2.1. 3D models and automated segmentation

We used model-assisted labeling (deep learning network predictions) to segment ten *Lobophyllia* colonies and five *Dipsastraea* colonies with a total of 4133 and 2511 zooid instances, respectively. The number of zooids per colony ranged from five to 2883 in *Lobophyllia* and 25 to 1911 in *Dipsastraea* (Fig. 2B, C). The size of each colony and number of zooids is detailed in (Fig. 2C and Table S1). Each zooid was classified primarily based on its shape representing its phase in the clonoparic cycle. In *Lobophyllia*, Single zooids are round shaped and typically have one mouth, Division type zooids are mostly eight shaped and have more than one mouth, and Multi-Division type zooids are irregularly shaped and have multiple mouths. When we started this research, we focused on zooid morphologies. We found that the relation between zooid shape and number of mouths was previously described by Matthai (1926), fitting our observations and supporting our classification scheme. In *Dipsastraea*, Late-Division zooids have a skeletal wall starting to form between mouths (see Fig. 3B). We only had six tri-stomodeal zooids from *Dipsastraea* in our data and we discarded them. The colony information is in Table S1.

2.2. Proportion of zooid types by colonies

To determine whether the proportions of zooid types (Single, Division, and Multi/Late Division) differed between colonies we performed a Chi-squared test with Monte Carlo simulations (10,000 iterations). In *Lobophyllia* (n = 10), the Division group did not show significant differences between colonies ($p = 0.9028$) with a mean of 0.50 ± 0.12. The Single and Multi-Division groups showed significant differences ($p < 0.005$) with means and standard deviations of 0.42 ± 0.15 and 0.077 ± 0.05, respectively. In *Dipsastraea* (n = 5), all groups showed significant differences between colonies ($p < 0.05$). The mean and standard deviation for the Single, Division, and Late-Division groups were 0.78 ± 0.05, 0.16 ± 0.03, and 0.025 ± 0.018, respectively. Test results are provided in Table S3.

2.3. Colony surface area and the number of zooids

The relationship between colony surface area and the number of zooids was modeled separately for *Lobophyllia* (n=10) and *Dipsastraea* (n=5) colonies using linear regression on log-transformed data (Fig. 2C). The slopes were 0.915 and 0.975 with intercepts of −2.595 and −3.373 for *Lobophyllia* and *Dipsastraea*, respectively ($p < 0.001$, $R^2 = 0.9785$ and 0.9836). The slope is slightly higher in *Dipsastraea* suggesting that it increases surface area more rapidly with zooid number than *Lobophyllia* colonies. The intercept difference of 0.778 on the log scale translates to: $10^{0.778} \approx 6.01$ resembling an approximate 6 times greater surface area in *Lobophyllia* colonies for the same number of zooids. The results are further detailed in Table S2.

2.4. Zooid size frequency distributions

To assess whether zooid perimeter is associated with developmental phase, we used linear mixed-effects models for each genus, treating developmental phase as a fixed effect and colony as a random effect.

For *Lobophyllia* ($n = 4133$), zooid perimeters varied significantly between developmental groups (Single, Division, and Multi-Division). The fitted median values for the 3D perimeter were 8.5 cm for the Single group ($n = 1,655$), 11.5 cm for the Division group ($n = 2,223$), and 16.3 cm for the Multi-Division group ($n = 255$). The Division group exhibited a significantly larger perimeter than the Single group ($\beta = 2.9942$ cm, $p < 0.001$), while the Multi-Division group showed an even larger increase in perimeter ($\beta = 7.8451$ cm, $p < 0.001$).

The perimeter differences between groups were substantial, with increases of approximately 3–5 cm between successive growth forms. In *Dipsastraea* ($n = 2510$), significant differences in zooid perimeter were also observed. The fitted median perimeters were 4.7 cm for the Single group ($n = 2,101$), 5.4 cm for the Division group ($n = 359$), and 6.1 cm for the Late-Division group ($n = 50$). Zooids in the Division group had larger perimeters than those in the Single group ($\beta = 0.6984$ cm,

[2] Zooids are meandroid and have their own walls (Veron et al., 2016).
[3] Change in rate or timing of development (Rougvie, 2013).
[4] Zooids from the same type grouped together in neighborhoods.
[5] A computer vision technique that identifies and distinguishes individual objects within a 3D scene while also segmenting them into distinct regions.
[6] Using predictions from a deep learning algorithm as suggestions for a human annotator.
[7] Non random clusters of zooids from the same developmental phase.

$p < 0.001$), and the Late-Division group had larger perimeter sizes ($\beta = 1.3789$ cm, $p < 0.001$). A post hoc test (we used Tukey contrasts for all post-hoc tests) showed significant differences in zooid perimeters among all developmental phase pairs (results are detailed in Table S5). Although there were significant differences in the 3D perimeter of developmental phases in *Dipsastraea* the changes were very mild (less than 1.5 cm), while for *Lobophyllia* the changes were more substantial at three-four centimeter difference (Fig. 3).

2.5. 3D perimeter of zooids by developmental phase vs colony size

To assess whether the total surface area of the colony is associated with 3D perimeter of zooids, we applied a generalized linear model for each genus with an interaction term between total surface area and developmental phase. In *Lobophyllia*, perimeter significantly decreased with increasing colony size in the Single group (n = 1,655, $\beta = -0.0023$, $p < 0.001$) and the Multi-Division group (n = 255, $\beta = -0.0054$, $p < 0.001$) but not in the Division group (n = 2223, $p = 0.673$). Despite these significant decreases, the magnitude of the perimeter reduction with increasing surface area was relatively small compared to the differences between groups. Specifically, the difference in perimeter between the Single and Multi-Division groups ($\beta = 0.0972$) was approximately 42 times larger than the effect of colony size in the Single group ($\beta = -0.0023$). Similarly, the difference between the Single and Division groups ($\beta = 0.0308$) was about 13 times larger than the effect of colony size.

In *Dipsastraea*, perimeter significantly decreased with increasing colony size in the Single group (n = 2,102, $\beta = -0.0028$, $p = 3.23 \times 10^{-5}$) and the Division group (n = 359, $\beta = -0.0089$, $p = 3.39 \times 10^{-8}$) but not in the Late-Division group (n = 50, $p = 0.363$). The difference in

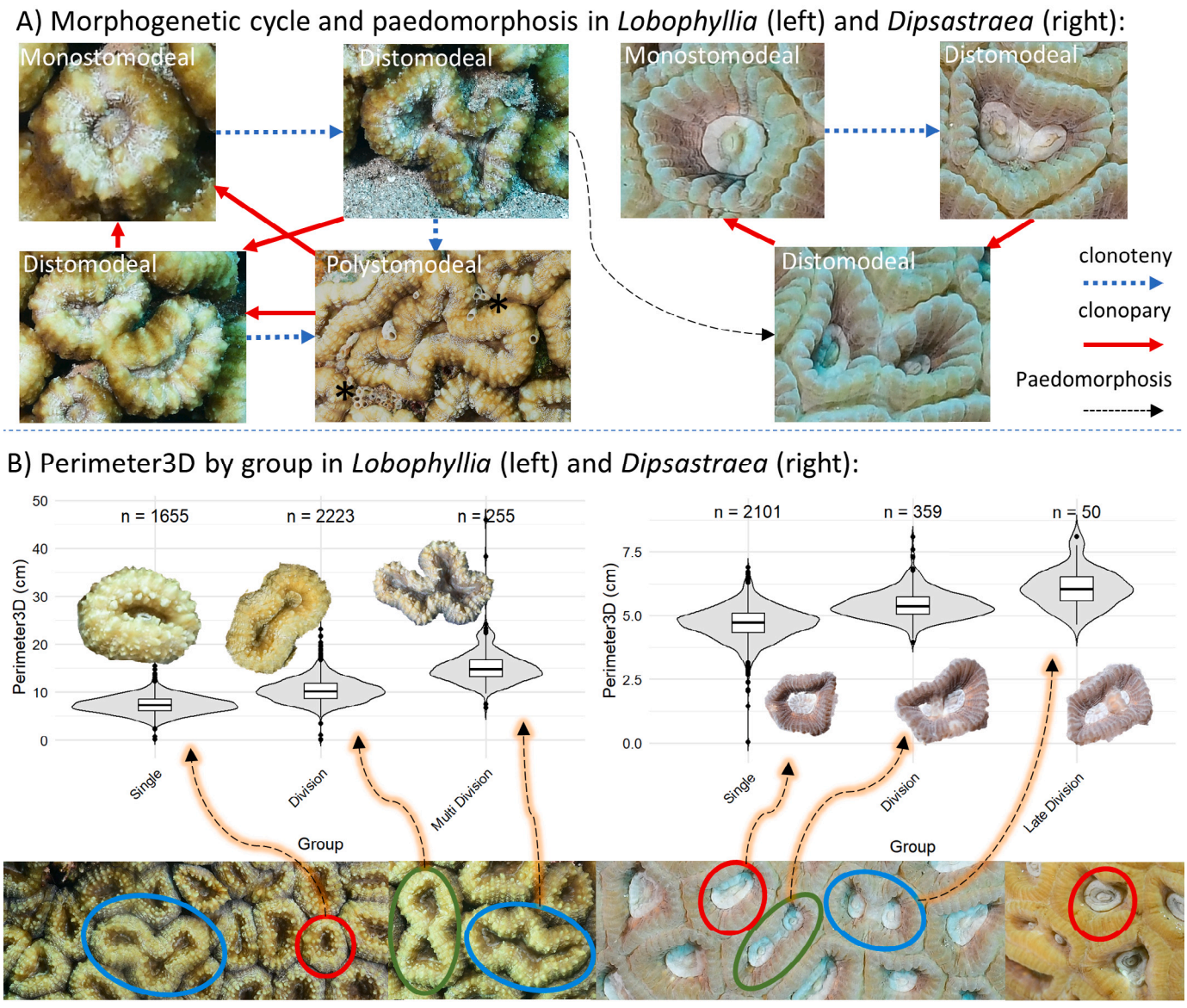

Fig. 3. Morphogenetic cycle in *Lobophyllia* and *Dipsastraea*: (A) Morphogenetic cycle and paedomorphosis in *Lobophyllia* (left) and *Dipsastraea* (right). The transitions between zooid types are illustrated, showing monostomodeal, distomodeal, and polystomodeal stages. The asterisks in the polystomodeal *Lobophyllia* zooid show overgrowth by vermetid gastropods in the cracks between zooids. A single monostomodeal zooid starts dividing until it is split into two or more zooids through clonoteny and clonopary. The arrows represent the possible pathways for zooid division, i.e., from distomodeal or polystomodeal back to monostomodeal. Blue dashed arrows represent clonoteny (addition of mouths within a zooid/polyp), red solid arrows indicate clonopary (separation of clones), and black dashed arrows highlight paedomorphosis (retention of juvenile traits in mature forms). (B) 3D perimeter analysis of zooids in *Lobophyllia* and *Dipsastraea* categorized into Single, Division, Multi-Division, and Late-Division developmental phases. Box and violin plots display the distribution of Perimeter 3D (cm) values, with sample sizes (n) indicated above each group. Significant differences were observed between all groups ($p < 0.001$). Representative zooids are outlined beneath the plots with arrows indicating their developmental phase.

perimeter between the Single and Late-Division groups ($\beta = 0.0144$) was approximately 5 times larger than the effect of colony size in the Single group ($\beta = -0.0028$). Likewise, the difference between the Single and Division groups ($\beta = 0.0110$) was around 4 times larger than the effect of colony size. These results indicate that although perimeter decreases with increasing colony size, the association between the developmental phase and perimeter is substantially larger. The results are detailed in Table S4.

2.6. Structural complexity from plane fitting vs. developmental phase

To examine the association between surface complexity and developmental phase we used mixed effect models with a binomial error distribution, testing transitions between each pair of groups separately (see methods 4.5 and Figs. 4, S5). In *Lobophyllia* structural complexity was associated with transitions between zooid groupings. The transition from Multi-Division (n = 255) to Single (n = 1,655) zooids showed the strongest negative association (estimate = −0.2396; S.E. = 0.0285; p < 2e-16). This suggests that single zooids are more common than Multi-Division zooids in areas of lower structural complexity. No significant associations were found for the transitions from Single to Division (n = 2223) zooids (estimate = −0.0025; S.E. = 0.0137;p = 0.854) or from Division to Single zooids (estimate = 0.0025; S.E. = 0.0137;p = 0.854). Interestingly, the transition from Division to Multi-Division showed a significant positive association (estimate = 0.2214; S.E. = 0.0286; p < 2e-16), implying that polystomodeal zooids are more likely to appear in structurally complex areas than distomodeal zooids.

In *Dipsastraea* Structural complexity had a strong negative association (Estimate = −0.30267, $p < 0.001$) on the transition from Single (n =2,101) to Division (n =359). A significant positive association (Estimate = 0.33884,p = 0.00114) was observed in the transition from Division to Late-Division (n =50). No significant association of structural complexity were found for the transition from Late-Division to Single. The results are detailed in Table S6.

These results support the idea that zooids employ the polystomodeal form in response to an increase in structural complexity. Nevertheless, some of the increase in structural complexity is generated by the shape of the zooid, which is generally more complex in polystomodeal zooids than their monostomodeal counterparts. To minimize this effect, we experimented with the threshold parameter of the plane fitting algorithm to find values that are least affected by the zooid's identity while still accounting for structural complexity in its vicinity. These measures are meant to buffer the effect of zooid identity on plane fitting (Fig. S5). We use a range of step-sizes aiming to detect structural features at different scales such as disturbance to the surface of the colony (small-scale) and objects in vicinity of the colony (large-scale).

To assess the association between colony size and zooid developmental phase with relation to structural complexity, we used generalized linear models (GLMs) with a binomial distribution using both structural complexity and the total number of zooids (Z-scored within each group) as predictors. We performed Z-score normalization of number of zooids within each group to avoid bias due to imbalance in size distributions across states. The results demonstrated that colony size had no significant association with any state transition in *Lobophyllia* or in *Dipsastraea* (Table S7).

2.7. Nearest neighbor interactions between zooids

By examining significant aggregation (right-sided tests) and segregation (left-sided tests) patterns across a range of nearest neighbors (K), we aim to understand the spatial interactions between different zooid developmental phases within colonies. Significant ($p < 0.05$) results are shown in Fig. 5 and Table 1, and all results are shown in Figure S3. In *Lobophyllia*, the Princess1 and Princess2 colonies exhibit strong autocorrelation in both the Single and Multi-Division classes, while segregation is observed from the Multi-Division to the Single class (Fig. 5, Table 1). In *Dipsastraea*, the most prominent findings included significant autocorrelation in the Single class and the Division class. These results suggest a combination of directional growth and stagnation.

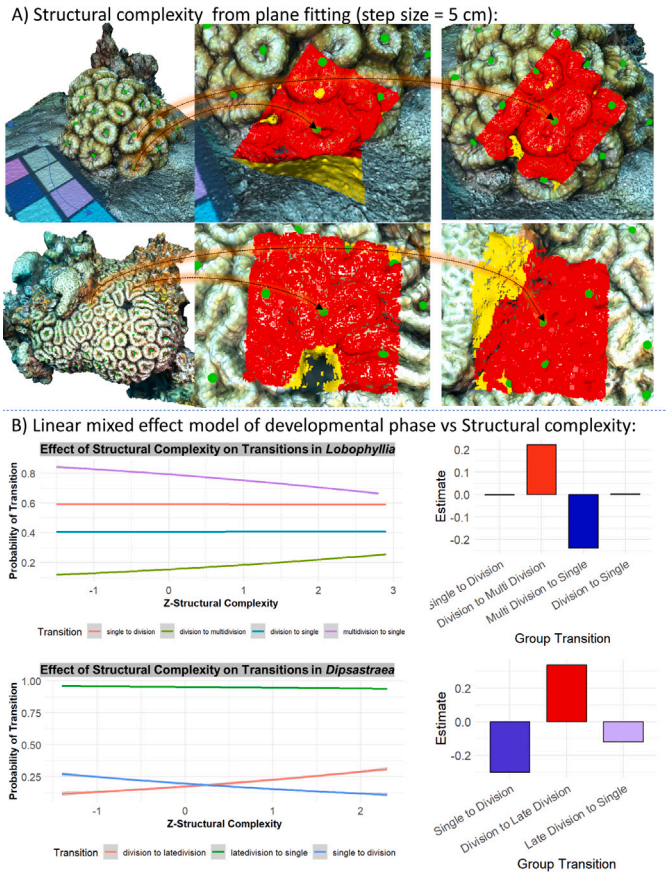

Fig. 4. Structural complexity association with growth phase: (A) Plane-fitting was used to calculate structural complexity around the center of each zooid (marked in green points, left). The top images show two colonies and close ups of the plane fitting at step-size 5 cm (the length of the cube used for plane fitting around the zooid is 5 cm) for zooids at the periphery, center of the colony, and near surface damage, showing that our algorithm is able to detect these as changes in structural complexity. Red points fit the plane and yellow points are outliers, complexity is calculated by the percentage of outliers. (B) The left images display the results of a linear mixed-effects model assessing the association between structural complexity and zooid developmental phase. Since these analyses evaluate transitions between two zooid types in a binary framework, the *y*-axis represents the probability of transitioning between developmental phases — indicating the likelihood of a zooid belonging to a specific developmental phase relative to its predecessor. The X axis is Z normalized structural complexity. In *Lobophyllia* (left) it is apparent that the transition to Multi-Division is associated with increasing curvature, and vice versa for the transition to Single (n= 2606, 1978; z-normalized scale, effect = 0.0245, −0.05; S.E. 0.0006, 0.0014; p < 2e-16, respectively). In *Dipsastraea* the transition to Late-Division is associated with increasing curvature, and vice versa for the transition to Single, although the effects are milder (n = 416, 2151; z-normalized scale, effect = 0.0155, −0.0205; S.E. 0.0007, 0.0009; p < 2e-16). The barplots on the left show the effect size (the slope of the curve) for each test.

To evaluate whether colony size is associated with likelihood of obtaining significant nearest neighbor aggregation, we conducted separate logistic regression analyses for each growth group: Single, Division, Late-Division, and Multi-Division. In each case, the probability of a significant result was modeled as a function of colony size using a binomial logistic regression. This analysis was performed by partitioning the data by developmental phase and testing for each (`From_Group`). Colony size was strongly associated with aggregation patterns in all groups except Late-Division in *Dipsastraea* (p = 0.08), with positive estimates indicating that more significant interactions occur with larger colony surface area. It is likely that these results are caused by the

Table 1
Significant ($p < 0.05$) results of nearest neighbor interactions, these results are displayed in Fig. 5, B. The left three columns summarize aggregation patterns (right-sided tests), and the right three columns summarize segregation patterns (left-sided tests). Each row corresponds to a specific cell in the NNCT, indicating the interactions within and between different zooid phases.

Right Sided Tests in Lobophyllia			Left Sided Tests in Lobophyllia		
From → To (Agg)	Colony (Agg)	K (Agg)	From → To (Seg)	Colony (Seg)	K (Seg)
Division → Division	Igloo2	1, 3	Division → Division	Igloo1	2
Division → Division	Princess2	7, 8	Division → Division	Igloo4	8–10
Division → Multi-Division	Igloo4	5, 7, 8	Division → Division	Kza1	3
Division → Multi Division	Kza1	3	Division → Division	Princess1	1–4
Division → Single	Igloo1	2	Division → Multi-Division	Princess1	1, 2, 7–10
Division → Single	Igloo3	4–7	Division → Multi-Division	Princess2	1
Division → Single	NR1	1	Division → Single	Igloo2	3
Division → Single	Princess1	1–5, 10	Division → Single	Princess2	6–10
Division → Single	Princess2	1	Multi-Division → Division	Igloo2	5, 6, 10
Multi-Division → Division	Princess1	7–9	Multi-Division → Division	Igloo4	5–7
Multi-Division → Division	Princess2	2–10	Multi Division → Division	NR2	9, 10
Multi-Division → Multi-Division	Princess1	6–10	Multi-Division → Single	Princess1	5–10
Multi-Division → Multi-Division	Princess2	4–10	Multi-Division → Single	Princess2	2–10
Multi Division → Single	Igloo4	5, 7	Single → Division	Igloo4	2–10
Multi-Division → Single	NR2	9, 10	Single → Division	Princess1	1–4, 9, 10
Single → Single	Igloo4	2, 3	Single → Division	Princess2	1–10
Single → Single	NR1	1, 2	Single → Multi-Division	Princess1	1–10
Single → Single	Princess1	1–10	Single → Multi-Division	Princess2	1–10
Single → Single	Princess2	1–10	–	–	–
Right Sided Tests in Dipsastraea			**Left Sided Tests in Dipsastraea**		
From → To (Agg)	Colony (Agg)	K (Agg)	From → To (Seg)	Colony (Seg)	K (Seg)
Division → Division	IUI1	8	Division → Division	Igloo1	1–3
Division → Division	IUI2	6, 8	Division → Division	Kza1	5, 6
Division → Division	Igloo1	8–10	Division → Single	IUI2	5–8
Division → Division	Igloo2	1, 6–9	Division → Single	Igloo1	8–10
Division → Single	Igloo1	1, 2	Division → Single	Igloo2	1, 5–9
Division → Single	Kza1	4	Late Division → Division	IUI1	5
Late-Division → Division	Igloo1	1	Late-Division → Single	Igloo1	1
Late Division → Late-Division	IUI2	1	Single → Division	IUI2	1
Late-Division → Single	IUI1	3–5	Single → Division	Igloo1	1–4, 9, 10
Single → Division	IUI1	2	Single → Division	Igloo2	1–5, 8–10
Single → Single	IUI2	1–3	Single → Late-Division	IUI2	2–5
Single → Single	Igloo1	1–5, 9, 10	Single → Late-Division	Igloo1	1–5
Single → Single	Igloo2	1–5, 7–10	Single → Late-Division	Igloo2	1, 4
Single → Single	Kza1	1, 2	–	–	–

significance in neighbor relations in the larger colonies (Princess1 and Princess2 in *Lobophyllia* and DipsIgloo1). The results are detailed in Table S8.

3. Discussion

We observed several main differences between phaceloid and cerioid colony forms: (1) Halting skeletal separation (colony remains in contact at the skeleton with polyps separated by walls), (2) a decrease in zooid size, and (3) disappearance of the undecided form: the flexible polystomodeal zooid, possibly via loss of arrested budding. These evolutionary shifts can be viewed as fine-tuning of the budding process and an optimization of the colony towards more compact and integrated structures. We saw that in *Dipsastraea* (cerioid) the polyps are more self-similar and homogeneous than in *Lobophyllia* (phaceloid) where the polystomodeal zooids are prevalent but also dividing zooids are more plastic with regards to their outlines (morphologies) and surface tiling capacity. Moreover, the surface area of colonies scales exponentially with the number of zooids for both genera with very similar rates, but the higher slope in *Dipsastraea* shows that the colonies are more compact, allowing for a faster increase in zooid number relative to the surface area. The flatter slope of *Lobophyllia* reflects a slower increase in zooid number, due to spacing between zooids. In the phaceloid structure, gaps form on the colony's surface deeming it vulnerable to predators and overgrowth (see Figs. 1, D and 3, B). On the other hand, skeletal separation provides an advantage as individual zooids can die off in case of disease without infecting neighboring zooids (Fig. 2, D) and without propagating damage throughout the colony (Simpson et al., 2020). One potential competitive advantage of the cerioid form is its enhanced compactness and symmetry in zooid organization around the mouths. The smaller zooids are possibly adaptive as the colony can accommodate, based on our results — six times more zooids within the same area (Results 2.3). Importantly, this reduction in zooid size does not lead to an equal decrease in mouth size. Instead, the zooids and colony structure become centered around the mouths, highlighting their critical role in key functions such as reproduction and metabolism.

The proportions of zooid types (Single, Division, and Multi-Division/Late-Division) varied notably between colonies except for the Division group in *Lobophyllia*. In *Dipsastraea* colonies, all three groups (Single, Division, and Late-Division) displayed significant differences between colonies. The low proportions of Late-Division zooids can be attributed to the slow nature of the division process. For example, Gateno and Rinkevich (2003) followed 190 polyps for three years and only 37 of them completed a full morphogenetic cycle (initiated and terminated budding). Importantly, they reported that the calcified wall separating the two mouths sometimes required up to two years to fully form from the date the second mouth was first recorded. Although the coral in that study was referred to as *Favia*, this species has since been reclassified as *Dipsastraea* following a later revision in taxonomy (Budd et al., 2012), making it extremely relevant to our observations.

The strong association of developmental phase and zooid size suggests that the morphogenetic cycle is size-dependent. This highlights the modularity of coral colonies, where zooids serve as building blocks that can be arranged in various configurations to produce high degrees of plasticity on the colony level. We also examined the association between colony surface area and zooid perimeter by type and found that although larger colonies tend to exhibit slightly smaller zooids in some

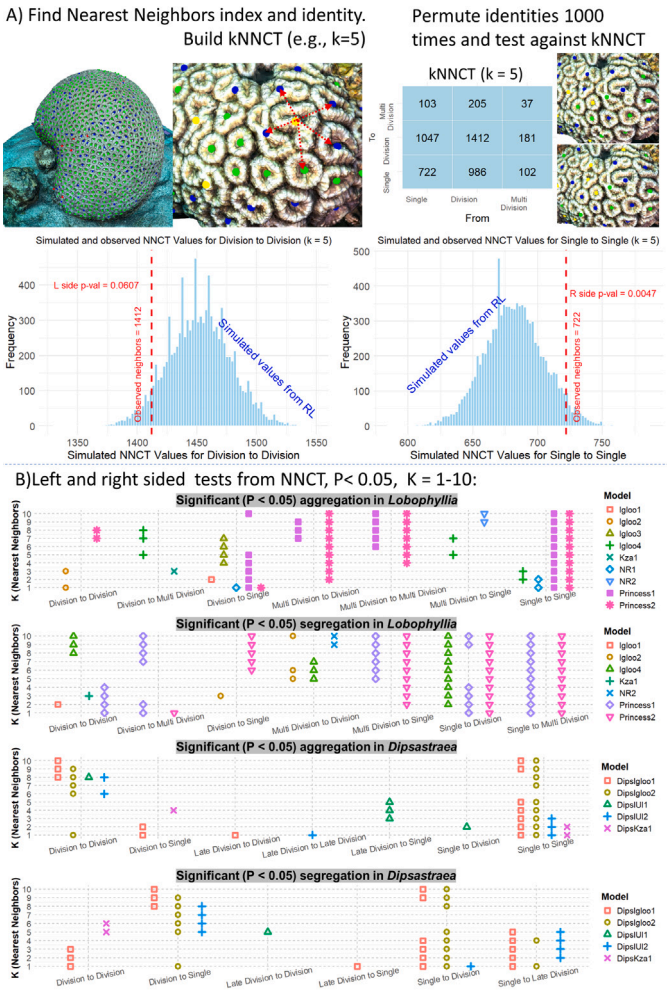

Fig. 5. Nearest neighbor interaction analysis for finding clusters of zooids from various types. (A) For a given colony the centroid and type of each zooid are recorded together with its k-nearest neighbors, to construct a nearest neighbor contingency table (NNCT, top-right), e.g., among the 5 nearest neighbors (NNs) of Division zooids 1412 are from Division zooids. In random Labeling (RL) the identity of each coral is permuted (see the colors are different in the sub images of A, right representing RL), and the NN relations are calculated to generate a distribution of simulated values. Bottom histograms show how a statistical test is conducted using the observed vs random labeled (RL) results. The red dashed line is the observed value from the NNCT, and the histogram is the simulated values from RL. We conduct this test over a range of k values (the number of neighbors from which the NNCT is built) to find at what neighborhood sizes, there are significant spatial interactions. The right-sided (aggregation) tests indicate where zooid types are spatially correlated, and the left-sided (segregation) tests show where zooids tend to repel each other. (B) The plots show aggregation (right-sided tests) and segregation (left-sided tests) for each genus, displaying only results where $p < 0.05$. The y-axis represents K nearest neighbors (K = 1–10), the x axis is the cells from the NNCT, colonies are marked in shape and color. For example, in *Lobophyllia* aggregation tests, the colonies Princess 1 and Princess 2 display significant aggregation in the Single-to-Single interaction over the full range of K (B, top right), and in *Dipsastraea*, DipsIgloo1 displays significant aggregation in the Division-Division interaction. The sample size (n) is colony specific and detailed in Table S1.

developmental phases, this effect was consistently small compared to the differences between developmental phases.

Corals begin their lives as single zooids (Fig. 1, A) and grow in an asymmetric environment — the benthos. They grow selectively towards, away from, or around the objects in the environment. A timelapse of the reef on decadal and centennial scales would reveal coral colonies moving purposefully around the seabed (Hughes et al., 2003; Marfenin, 1997), modifying it in the process (Jones et al., 1994; Lartaud et al., 2016). Thus, budding mechanics are not only a means of growth but also a means of slow movement or colony-scale locomotion. Although our observations and results represent a snapshot in time and time-series data is hard to obtain, we view budding as a slow and continuous process that can involve periods of stagnation and can have different rates throughout the colony and across colonies (Gateno and Rinkevich, 2003). Primarily, as we show here, the size of zooids is conserved, meaning that zooids in large colonies are a product of budding. However, there can be advantages for zooids and colonies to remain stagnant. For example, visual observations led us to believe that when *Dipsastraea* colonies encounter obstacles such as rocks, they stop growing in the vicinity of it and increase growth on the opposite side. This strategy results in overgrowing the obstacle in the long term since zooids are connected at the skeleton and the colony maintains a close-to-spherical shape.

Our results in the nearest neighbor experiment (Fig. 5) show that in the colony DipsIgloo1, which is the biggest *Dipsastraea* colony in the dataset and has a rock next to it, there were significant coalitions of Single zooids indicating stagnation, and significant coalitions of dividing zooids indicating directional growth. In *Lobophyllia*, aggregation patterns were significant. Notably, Single and Multi-Division zooids exhibited autocorrelation in the largest colonies, indicating directional growth and stagnation. While our results successfully identify aggregation and segregation patterns, they do not provide spatial context for where these patterns occur on the colony surface. An important follow-up study would involve mapping the spatial distribution of coalitions by assigning segregation/aggregation scores to each zooid and comparing these scores with local structural complexity.

The polystomodeal undecided form occurs by heterochrony in the budding process (Pandolfi, 1988), where several budding processes occur at different times and rates in the same zooid (a new budding event starts before the previous ends) giving rise to strangely shaped outlines — the undecided form. This zooid is competitive and potentially adaptive — characterized by multiple mouths and remarkable shape plasticity that enables it to fit tightly into restricted spaces and fill in voids on the colony's surface. One of our main hypotheses is that corals employ this morph to deal with external and internal disturbances and to compete for space (Figs. 1, D, 2, A). We did not manage to explicitly answer this question, however our findings align with the hypothesis that budding dynamics are associated with structural complexity and that the undecided form is associated with higher structural complexity such as in colony edges or regions with surface disturbances (e.g., missing zooids on the surface of the colony Figs. 4, S2). *Lobophyllia* has much more flexibility in growing around objects and filling voids on the colony's surface by employing the undecided form and differential budding. This is a unique example of surface tiling, an important phenomenon in the natural world (Domokos et al., 2024). Corals provide valuable insights on complex tessellation tasks, and an important follow-up study would focus on linking the polystomodeal zooids more explicitly to surface tiling in *Lobophyllia*, particularly examining their distributions in relation to gaps in the surface of the colony.

We found six tristomodeal zooids in *Dipsastraea*. This was surprising because these corals usually cycle between one and two mouths (Figs. 1,2). Although they were polystomodeal, they were not as flexible as the polystomodeal phaceloid zooids (undecided form in *Lobophyllia*). The cerioid *Dipsastraea* is fully connected by tissue and skeleton, and is thus less likely to require the undecided form for complex tessellation (surface tiling) tasks. The undecided form in *Lobophyllia* can be viewed as a polymorphic zooid that enhances the plasticity of the colony and can drive the emergence of new colony forms (Simpson, 2021). For example, when flabello-meandroid traits are combined with the compactness of cerioid forms by maintaining multi-stomodeal zooids in a skeletally intact structure, the resulting colony adopts a meandroid form, as seen in genera such as *Gyrosmillia*. Therefore, meandroid colonies may have evolved through paedomorphosis, where a polystomodeal phaceloid ancestor lost its pseudo-colonial traits in favor of a

compact and fully integrated skeletal structure (Pandolfi, 1992; Rosen, 1986).

Corals are traditionally thought to exhibit limited polymorphism in their zooids compared to other benthic colonial organisms (Simpson et al., 2017). Nevertheless, in some coral genera zooid specialization and division-of-labor are distinct. For example, in *Acroporids*, terminal zooids in branches remain terminal throughout their life, and functional compartmentalization occurs within colonies (Shmuel et al., 2022). Furthermore, functional diversity in a colony typically increases when not all group members are reproductive (Simpson, 2012). An interesting follow-up study would investigate whether polystomodeal zooids, (which represent functionally diverse units) exhibit distinct roles, for example, if they differ in fecundity from monostomodeal zooids.

Matthai (1926) argued that the coral colony must be regarded as the individual, and Brickner et al. (2006) showed self vs. non-self recognition in *Lobophyllia*. Zooids in a colony are considered clones but mutations are likely accumulated. Moreover, fragmentation (e.g., Fig. 1, D) is known to be an important means of reproduction and dispersion in corals (Highsmith, 1982; Hughes and Jackson, 1985). Considering the longevity of corals, in the long run, the columnar phaceloid corallites of *Lobophylliia* are broken off and dispersed by storms, waves, and currents. If not, they will break under their own weight (Jones, 1907, Fig. 1, D). When zooids break from the colony, they pioneer new colonies and even merge back with their source colonies, resulting in large mono-specific carpets or even carpets of individual (see above on the colony as an individual) genotypes rather than large boulder colonies of the massive morphology. Studying the extent of genetic drift in a colony and the genetic similarity of zooids in mono-specific reef patches is an interesting avenue for future research.

Symbiosis is an important factor in coral evolution (Stanley Jr., 2003; Stanley Jr. and Van De Schootbrugge, 2009). The presence of symbiotic microalgae in corals correlate with colony integration (i.e., distance and skeletal separation between zooids) and a decrease in zooid size (Coates and Jackson, 1987; Hughes et al., 2003), similar to the phaceloid-cerioid transitions. A possible scenario is that large ancestral zooids acquired symbiotic algae and evolved into smaller zooids and more integrated colony forms, i.e., cerioid (Hughes, 1983). Nevertheless, a recent study showed that corals with and without symbiotic micro-algae co-existed on ancient reefs as they do today (Jung et al., 2024). Although we did not sample the microalgae in these corals or measure their photosynthetic profiles, an interesting follow-up work will focus on correlating photosynthetic activity and zooid dynamics. Trophic strategy is broadly linked with polyp size, with large pseudo-solitary (e.g., phaceloid) zooids considered more heterotrophic and integrated coral colonies considered more autotrophic (Coates and Jackson, 1987). Moreover, heterotrophy plays a major role in skeletal growth (Houlbrèque and Ferrier-Pagès, 2009), and an interesting follow up study will measure the trophic levels of zooids to test if polystomodeal zooids are more heterotrophic than monostomodeal zooids.

Depth affects corallite structure (Kramer et al., 2022), perhaps as a result of light or nutrient availability. For example, it has been shown that corallite diameter of a Caribbean coral decreases with depth (Studivan et al., 2019) while another study showed that these trends are not consistent between species (Doherty et al., 2024). Here we focused on a narrow depth range of 3–9 m. The depth dependence of zooids should now be quantifiable in situ for colonies photographed along a depth gradient and an interesting follow-up work will implement our methods on a depth gradient.

This is the first work to study thousands of coral zooids in situ using 3D imaging and deep learning. Nevertheless, it has several limitations that are important to consider when interpreting the results. First, we report descriptive results of a temporal process — the morphogenic cycle, sampled across space. This space-for-time substitution (Lovell et al., 2023) has been useful in coral ecology for example for describing anthropogenic effects on benthic communities (Smith et al., 2016). Although it has benefits in describing slow processes such as atoll formation by subsidence (Darwin, 1889; Woodroffe, 2011), it is also criticized in ecological studies and it is recommended to complement large spatial datasets with sparse temporal data (Damgaard, 2019). Our results document associations rather than direct causal effects. An aquarium experiment focused on budding mechanics would complement that, for example on zooid reaction to structural complexity. Secondly, our classification scheme is based primarily on morphology and not strictly on the number of mouths. When we started this work, our focus was on describing morphological dynamics within the morphogenetic cycle and only later, we realized the role of mouths for classic zooid classification. Nevertheless, our observations are consistent with earlier descriptions linking between zooid shape and number of mouths (Matthai, 1926), supporting our classifications scheme. However, a more rigorous classification scheme would identify the number of mouths and zooid morphology. Another limitation of this study is the potential for pseudo-replication due to the spatial proximity of sampled coral colonies. While we made efforts to visually distinguish and sample independent colonies, without genetic data we cannot fully exclude the possibility that some colonies are a product of fragmentation and are the same genotype. Furthermore, genotyping (e.g., Capel et al., 2025) would provide a reliable method to confirm species identity particularly in genera with cryptic diversity.

A recent review on the role of modularity in coral growth highlighted that understanding the fundamental rules of coral clonal growth is essential for improving predictions of coral reef recovery and guiding restoration efforts (Re et al., 2024). While significant progress has been made, such as the development of growth models based on polyp cloning (Llabrés et al., 2024), these models lack validation through in situ observations of zooid dynamics.

This gap underscores the importance of our work, which represents the first study to examine budding mechanics in situ on thousands of zooids. A previous study highlighted the potential of underwater imaging to study zooid dynamics (Todd et al., 2001), here we use state-of-the-art technology based on underwater imaging to achieve that. By providing empirical data on the spatial organization and size distribution of coral zooids, this study addresses a critical gap for understanding modular growth under natural conditions. For instance, understanding how budding mechanics and modularity affect resilience in corals can help to inform strategies for reef restoration and conservation. The segmentation-based approach developed here could be applied to track zooids over time, offering a novel tool to study coral growth dynamics in nurseries and in the wild. Moreover, it can be used to provide demographic rates accounting for variability within colonies. This kind of novel information is important for predicting the trajectories of ecosystems under global change (Dornelas et al., 2017).

Coral reefs are some of the most diverse and intricate ecosystems on the planet, however they are extremely sensitive and vulnerable to the adverse effects of climate change and anthropogenic impacts (Hughes et al., 2017). Understanding their dynamics in a bottom up-way can help to mitigate these threats by revealing the mechanisms that drive coral colony formation, and shed light on patterns of reef resilience, which vary within and between colonies. Furthermore, the dataset released here includes the segmentation outline of individual zooids, offering a valuable resource for studying natural tiling patterns, that can enrich research and applications ranging from bio-inspired design and architecture to modeling growth in modular, colonial organisms.

4. Methods

4.1. 3D imaging

We captured overlapping images of each coral using a Nikon DSLR camera (45 MP, JPG-fine) and underwater strobes. Camera settings

and strobes were adjusted for sharp, well-lit images. Using the camera's intervalometer, images were taken at one frame per second with 50%–80% overlap while swimming around the colony at distances of 0.3 m and 1 m.

3D models were processed in Agisoft Metashape (Agisoft Metashape Professional, Version 1.8, Agisoft LLC, St. Petersburg, Russia, 2016.) with high-accuracy photo alignment and adaptive camera model fitting. We ensured model quality by using high-accuracy photo alignment with adaptive camera model fitting and generating meshes from high-quality depth maps with low face counts to minimize noise and enhance processing efficiency. The images were captured at a resolution of 45 megapixels (JPG-fine format).

Models were scaled directly in Metashape using at least two DGK color cards per model, each measuring 20 cm in length. Consistent selection of distinct points on the scale bars across multiple images reduced scaling error to below 0.0005 m, ensuring accurate model dimensions. Cropped models were exported in PLY format for further analysis.

4.2. Sampling schematic and data-set

The data used in this study contains ten models of *Lobophyllia* and five models of *Dipsastraea*. The models were captured in Eilat at depths of 3–9 m. The coral models were collected from multiple dive sites along an approximately 4 km stretch of coastline near the Interuniversity Institute for Marine Sciences of Eilat. The sites were selected for their accessibility from the Interuniversity Institute for Marine Sciences of Eilat and included Princess Beach (two *Lobophyllia* colonies), the Interuniversity Institute (one *Lobophyllia* colony, two *Dipsastraea* colonies), Nature Reserve (two *Lobophyllia* colonies) and Underwater Observatory (Igloo, four *Lobophyllia* colony, two *Dipsastraea* colonies), and Kazaa Oil Jetty (one *Lobophyllia* colony, one *Dipsastraea* colony). In each site the colonies were spaced at least ten meters apart. We chose the colonies haphazardly, while diving and looking for suitable colonies that can be easily imaged from all angles. Colonies were identified visually in situ by their distinct morphological features (Veron et al., 2016), *Dipsastraea* was identified by its cerioid form, characterized by clearly separated zooid walls, while *Lobophyllia* was recognized by its distinctive flabello-meandroid shape. Identifications were verified from the high-resolution images.

The *Lobophyllia* colonies likely belong to the species *Lobophyllia corymbosa*, though definitive identification requires molecular analysis. Similarly, the *Dipsastraea* colonies are likely *Dipsastraea veroni*, which is easy to distinguish based on its beehive structure, but this also cannot be confirmed without molecular data. Previous research (Rachmilovitz et al., 2022) identified two *Lobophyllia* species and nine *Dipsastraea* species in the region using a molecular analysis. It is possible that some of the *Lobophyllia* colonies are from the species *hemprichi*, but that does not affect the genera level analysis because they have similar morphological traits (Veron, 1986).

The surface area and number of zooids of each type per colony are summarized in Table S1. Surface area was calculated using Metashape's in built function after trimming the model to contain only the focal colony. The number of zooids was determined after completing the 3D instance segmentation via model assisted labeling and manual validation of each segment (zooid). The number of zooids and their types was extracted as the list of shapes in the 3D model. Models were exported in PLY format for further structural complexity analysis.

4.3. Classification

The zooids were classified primarily based on their morphology, reflecting their number of mouths, and representing their phase in the morphogenetic cycle. In *Lobophyllia*, Single zooids are round shaped and typically have one mouth, Division type zooids are mostly eight shaped and have more than one mouth, and Multi-Division type zooids are irregularly shaped and have multiple mouths. When we started this research, we focused on zooid morphologies. We found that the relation between zooid shape and number of mouths was previously described by Matthai (1926) fitting our observations and supporting our classifications scheme.

Initially, five categories were used for *Lobophyllia*: Single, Early-Division, Mid-Division, Late-Division, and Multi-Division. For the final analysis, these were consolidated into three broader categories: Single, Division (combining Early, Mid, and Late-Division), and Multi-Division. A similar merging approach was applied to *Dipsastraea*, merging Early-Division and Mid-Division as the Division class. In *Lobophyllia*, classification primarily relied on the shape of the zooid and number of mouths. If the mouths were not clearly visible, the zooid was classified based on the shape of its calice where dividing zooids had mostly an 8 shaped skeleton and Multi-Division zooids had a flexible outline with multiple concurrent budding events. For *Dipsastraea*, the Late-Division stage was defined by the presence of a mild skeletal ridge partially separating the calices in the distomodeal zooid, although they were not yet fully divided. The decision to merge categories aimed to simplify the analysis while retaining biologically relevant distinctions between single, dividing, and polystomodeal zooids. This approach reduced classification ambiguity and focused the analysis on major developmental phases rather than subtle intermediate stages.

For automated semantic segmentation we used the Detectron2 network (Mask RCNN) using the standard settings suggested in Wu et al. (2019) (IMS_PER_BATCH: 16, BASE_LR: 0.02, MAX_ITER: 90000, the settings are detailed here: https://github.com/facebookresearch/detectron2/blob/main/configs/Base-RCNN-FPN.yaml and our code for training is available here: https://github.com/VISEAON-Lab/mal-coral/blob/master/train.py.). We trained the network in two stages. In the first stage, using 60 partially annotated images with 1617 annotations in 5 unbalanced classes. These were annotated in Labelbox (Labelbox, online, 2023. https://labelbox.com) by experienced marine biologists. Then, the trained network was used for instance segmentation on 105 new images of other coral colonies. This output was used as suggested label predictions for confirmation by a human annotator, resulting in 9040 annotations in five unbalanced classes (5065, 1727, 1235, 803, 212). These were used to train the final model of the network, which was used to predict the zooid segmentation for the remaining 3D models. For each model, we selected a series of images that show all the zooids from multiple views. These images were used as input for the final model of the network. In this way, each zooid is identified and delineated several times as it appears in several images. Then, we use the 3D model to unify overlapping segments and obtain an instance segmentation where each zooid is counted only once. To summarize, Labelbox platform was used for validating and refining the network predictions. We then used the validated labels to train the network again. Then we used the network for predicting the instance segmentation and validated the classifications and segments after projecting the labels to the 3D model.

4.4. 3D instance segmentation

Although we used an algorithm for assisted labeling to segment and classify zooids, all segmentation results were manually validated in 3D to ensure accuracy. Model-assisted labeling refers to a semi-automated process where a machine learning algorithm aids in annotation tasks. In our case the deep neural net provides segmentation and classification of zooids which are validated by a human annotator. The algorithm generates pixel-wise masks for each zooid, which are then converted into vector-based polygons. These polygons are projected onto the 3D model and unified to create coherent 3D segments. Despite its efficiency, the algorithm is not flawless and requires manual validation to address two primary sources of error: inaccuracies in 2D classification and segmentation and errors during 3D projection.

Certain zooids were not reconstructed well in the 3D models due to occlusions or limited views such as on the bottom side of colonies. These situations are detailed in Fig. S4 where some zooids were not delineated. However, these cases represent only a small fraction of the dataset.

The algorithm for 3D instance segmentation takes a series of multi-view images where the zooids are identified in each image, projects the labels, and unifies them. We use 2D annotations (whether they are manually created or generated by a neural network) from multiple images.

The labeling consists of instance segmentation, where every object in the images (zooid) is delineated and classified. This results in multiple labels for the same object since each zooid is viewed in several images from different angles.

We projected the labels to the 3D model and automatically merged overlapping shapes from the same class. To project the labels, merge, filter, and clean them, we developed a custom Python script and deployed it from the Metashape console. Our code is available online at https://github.com/VISEAON-Lab/mal-coral.

Labels predicted by the network were converted from pixel-wise masks into vector-based polygons and simplified using the Douglas-Peucker algorithm from the Shapely Python library to reduce noise while preserving essential structural details. This step helps to simplify polygons by reducing the number of vertices while preserving its shape. Points were further filtered based on projection errors to improve the accuracy of the segmentation. We calculate the projection error by measuring the distance between each two successive points in each polygon in 2D and in 3D, and calculate the ratio of distances. Points that had a mismatch in their 2D and 3D distances were removed using a threshold of 0.00025 (chosen empirically). This step selectively removed geometric artifacts that often occur when segmenting complex or over-smoothed contours, especially in zooids with convoluted outlines. This helps refine the outline around wiggly zooids. On average, the resulting 3D polygons contained 43 vertices for *Lobophyllia* and 23 vertices for *Dipsastraea* (Fig. S4).

Next, polygons belonging to the same class were checked for overlap and cleaned. This process continues until we finish iterating over all the images (and all inner-class intersections were removed). However, there may still be cases of misclassification where zooids are annotated with different polygons belonging to other classes due to network errors. To address this, the class with the highest total confidence is selected. Finally, before exporting, the 3D model and labels were manually inspected, corrected, and cleaned to ensure the segmentation quality.

The 3D center of each shape was calculated by first determining the centroid of the 2D polygon and then projecting this point back into 3D space. This approach ensures that the computed center lies within the corresponding segment of the 3D model. The 3D polygon labels were exported as sets of X, Y, and Z coordinates clipped to the vertices of the 3D model. These coordinates were subsequently utilized for further analysis in Python and R. The accompanying dataset includes these exported values for reference.

4.5. Structural complexity from plane fitting

This analysis investigates the impact of local structural complexity on the developmental phase of each zooid. We hypothesized that coral colonies employ budding in response to changes in structural complexity and expected to observe a higher proportion of dividing and polystomodeal (Multi-Division class) zooids in areas with increased structural complexity. To model transitions between growth phases within the morphogenetic cycle, we applied a binary model that captures phase changes.

To quantify the local structural complexity around the center of zooids, we implemented a plane-fitting method at multiple spatial scales. We used several scales (step-sizes) to detect structural features ranging from small-scale disturbances on the colony surface to larger physical objects at the colony border. For each zooid (n = 4133/1655, *Lobophyllia/Dipsastraea*), at each step-size (3–18 cm), a cubic subset (the cube side length is the step-size) of the 3D model was extracted around its center (see methods 4.4 for further explanation on centers). The vertices of the mesh that fell within this cube were extracted as a point cloud which was used for plane fitting.

The plane-fitting function from the Open3D Python library was used to fit a plane to the point cloud using the Random Sample Consensus (RANSAC) algorithm with $n = 3$, where n is the number of randomly selected points used to define the plane. The algorithm iteratively refined the fit over 1,000 iterations. Points within a predefined distance threshold of 0.005 were considered inliers (aligned with the plane), and points beyond this threshold were classified as outliers. This threshold was empirically chosen to balance sensitivity to surface complexity generated by the zooid to that from its environment. The structural complexity score was calculated as the percentage of outlier points relative to the total number of points in the cube:

$$\text{Complexity Score} = \frac{\text{N (outlier points)}}{\text{N (total points)}} \times 100 \quad (1)$$

This measurement was repeated 30 times for each zooid at each scale to account for variability due to the random selection of points, and the average complexity score was recorded. A flat surface fits a plane with few or no outlier points, whereas a rugged and complex surface results in more outliers. Therefore, the percentage of outlier points reflects the structural complexity of the area around each zooid's center. We fitted planes at several scales by incrementing the cube length by 1 cm, starting from 3 cm up to 18 cm. This plane-fitting method effectively captures subtle surface variations and provides a reliable measure of local structural complexity (see Figs. 4, S5).

4.6. Nearest neighbors spatial interaction analysis

This analysis tests whether zooids form spatial clusters by developmental phase within a colony, which may indicate directional growth, such as clusters of dividing zooids. We employed a k-Nearest Neighbor Contingency Table (k-NNCT) approach to evaluate spatial interactions, including clustering and segregation patterns, among zooid types.

The k-NNCT is constructed based on Euclidean distances between zooid centers and their identities (i.e., types). For each zooid (referred to as the base type), the k nearest neighbors are identified, and their types are recorded. A contingency table is created from the base zooid types and the types of their k-nearest neighbors. Observed and expected frequencies are computed for each table entry (cell), where "cells" represent specific pairwise interactions between zooid types.

To test for significant clustering or segregation, we performed cell-specific permutation tests. Zooid identities were permuted 1,000 times, and a new k-NNCT was generated at each iteration. For each cell, the observed count was compared to the distribution of permuted counts to compute two-sided p-values: Right-sided tests identify clustering, where zooid types are observed together more frequently than expected by chance. Left-sided tests detect segregation, where zooid types are observed together less frequently than expected.

This method was applied over a range of k values ($k = 1, 2, \ldots, 10$) to capture both immediate neighbors and higher-order interactions. Since the large sample tests are only available for k=1 we resort to permutation versions for k-NNCT for k> 1. Along this line, we permute the identities (i.e., types) of zooids at each iteration, constructing a new k NNCT based on the permuted labels (of the zooid types). For each cell, we compare the permuted cell (i.e., entry) count to the observed count. We then calculate a p-value as the proportion of times permuted values are larger (smaller) than the observed count for the right (left) sided alternative, where p-values are indicative of positive spatial correlation or segregation for the cells (Ceyhan, 2009; Dixon, 1994).

4.7. Statistical analysis

Analyses were conducted using the R Statistical language (version 4.2.2; R Core Team, 2022).

Surface Area vs. Number of Zooids: To evaluate the relationship between colony surface area and the number of zooids we applied a linear regression model with log-transformation. Separate models were fitted for *Lobophyllia* and *Dipsastraea* colonies

Type Frequency Distributions: To analyze the frequency distribution of zooid types (developmental phases), we calculated their proportions within each colony and tested each group separately using a chi-squared test. For each group, the observed proportion was compared to the combined proportion of all other groups (1-Prop). A Monte Carlo simulation with 10,000 iterations was used to assess whether the proportions of zooid types differed significantly between colonies.

Size frequency distributions: We applied a linear mixed-effects model using colony as a random effect and zooid type as grouping factor and subsequently performed a post-hoc test using Tukey's correction. We chose colony as a random factor to account for between colony variation.

```
model <- lmer(Perimeter3D ~ group + (1 | colony))
posthoc <- glht(model, linfct = mcp(group = "Tukey"))
```

To evaluate if the effect of surface area on perimeter varied across developmental groups (Single, Division, Multi-Division/Late-Division) we fitted a linear model with colony surface area (`TotalSA`) and zooid group as predictors including their interaction term:

```
model <- lm(perimeter3D ~ TotalSA * group)
```

Zooid type vs structural complexity: First, we assigned a binary column to each zooid type. Next, we subset the data by selecting two groups at a time, based on their biological order. We specifically chose each zooid type and tested its effect against its predecessor type. To illustrate, let us consider the association between structural complexity and the occurrence of dividing zooids. We narrowed down the dataset to include only Single and Division zooids. We then utilized the binary column representing dividing zooids as the response variable in a generalized mixed-effects model with both structural complexity and step-size normalized using z-scores:

```
model <- glmer(Single to Division ~ structural
 complexity_z * step-size_z + (1 | colony)),
family = binomial)
```

Here, step-size represents the side length of the cube used for plane fitting. This model allowed us to evaluate how structural complexity and spatial scale jointly affect the likelihood of zooid division. To examine the association between colony size and developmental phases, we applied a generalized linear model (GLM), where both structural complexity and total zooid counts were standardized (z-scores). Importantly, total zooids were normalized within each group separately to account for imbalances in group sizes.

```
model <- glm(Group ~ structural complexity_z
 + TotalZooids_z, family = binomial)
```

This model tested whether colony size and local structural complexity was associated with the developmental phase distribution of zooids.

Nearest Neighbor significance by colony size: To examine the association between colony surface area on the likelihood of observing significant spatial clustering among zooids, we fitted a Generalized Linear Model (GLM) with a binomial distribution. In this model, the response variable was binary indicating whether a spatial interaction was statistically significant ($P\_Value \leq 0.1$) from any group. We then modeled the effect of the normalized colony surface area on the probability of significant clustering using the following GLM:

```
model <- glm(significant transitions ~ TotalSA,
 family = binomial)
```

This model allowed us to assess whether larger colony surface areas are associated with a higher or lower likelihood of significant spatial clustering or segregation among zooids.

CRediT authorship contribution statement

Matan Yuval: Writing – review & editing, Visualization, Project administration, Investigation, Formal analysis, Conceptualization, Writing – original draft, Validation, Methodology, Funding acquisition, Data curation. **Amit Peleg:** Writing – review & editing, Software, Formal analysis, Visualization, Methodology, Conceptualization. **Elvan Ceyhan:** Methodology, Writing – review & editing, Conceptualization. **Dan Tchernov:** Conceptualization, Writing – review & editing. **Yossi Loya:** Conceptualization, Writing – review & editing. **Avi Bar-Massada:** Methodology, Conceptualization, Writing – review & editing, Formal analysis. **Tali Treibitz:** Supervision, Conceptualization, Writing – review & editing, Funding acquisition.

Declaration of Generative AI and AI-assisted technologies in the writing process

During the preparation of this work the authors used chatGPT in order to create figures in R and edit several sections of the manuscript. After using this tool/service, the authors reviewed and edited the content as needed and take(s) full responsibility for the content of the publication.

Funding

T.T. was supported by the Leona M. and Harry B. Helmsley Charitable Trust, the Maurice Hatter Foundation, the Israel Ministry of National Infrastructures, Energy and Water Resources Grant 218-17-008, the Israel Ministry of Science, Technology and Space grant 3–12487, and the Technion Ollendorff Minerva Center for Vision and Image Sciences. M.Y. was supported by the Data Science Research Center at the University of Haifa, the Murray Foundation for student research, and Microsoft AI for Earth; AI for Coral Reef Mapping, and the Rohr Foundation. This research was supported by the Israel Data Science Initiative (IDSI) of the Council for Higher Education in Israel and the Data Science Research Center at the University of Haifa.

Declaration of competing interest

The authors declare that they have no known competing financial interests or personal relationships that could have appeared to influence the work reported in this paper.

Acknowledgments

We thank Alan Foreman for important edits and constructive comments, and Yoav Avrahami and Shlomi Vainer for a constructive critical read. We thank the Interuniversity Institute for Marine Sciences of Eilat for making their facilities available to us. We thank Aviad Avni and Opher Bar-Nathan for valuable intellectual and technical contributions, Fred Bosire and Eran Shviro for help in image annotations, Gal Eyal for help with producing the image in Fig. 1, D; Fieldwork in Eilat was carried out under permit 42–128 from the Israeli Nature and Parks Authority. The authors declare no conflict of interest.

Appendix A. Supplementary data

Supplementary material related to this article can be found online at https://doi.org/10.1016/j.ecoinf.2025.103293.

Data availability

The data used in this study (zooid perimeters, centers, and structural complexity calculations) is available at https://doi.org/10.5281/zenodo.14783315, the code used for structural complexity analysis, statistical analysis, and creating the figures is available at: https://github.com/MatanYuval/ReefMetrics/tree/main/ZooidSeg, the code for model assisted labeling is available at: https://github.com/VISEAON-Lab/mal-coral.

References

Brickner, I., Oren, U., Frank, U., Loya, Y., 2006. Energy integration between the solitary polyps of the clonal coral Lobophyllia corymbosa. J. Exp. Biol. 209 (9), 1690–1695.
Budd, A.F., Fukami, H., Smith, N.D., Knowlton, N., 2012. Taxonomic classification of the reef coral family Mussidae (Cnidaria: Anthozoa: Scleractinia). Zool. J. Linnean Soc. 166 (3), 465–529.
Capel, K., Ayalon, I., Simon-Blecher, N., Zweifler Zvifler, A., Benichou, I.J., Eyal, G., Avisar, D., Roth, J., Bongaerts, P., Levy, O., 2025. Depth-structured lineages in the coral Stylophora pistillata of the Northern Red Sea. NPJ Biodivers. 4 (1), 13.
Ceyhan, E., 2009. Overall and pairwise segregation tests based on nearest neighbor contingency tables. Comput. Statist. Data Anal. 53 (8), 2786–2808.
Coates, A.G., Jackson, J.B., 1987. Clonal growth, algal symbiosis, and reef formation by corals. Paleobiology 13 (4), 363–378.
Damgaard, C., 2019. A critique of the space-for-time substitution practice in community ecology. Trends Ecol. Evolut. 34 (5), 416–421.
D'Arcy, W.T., 1942. On growth and form. Camb. Univ. Press 1 (6), 7.
Darwin, C., 1889. The Structure and Distribution of Coral Reefs. vol. 15, D. Appleton.
Dixon, P., 1994. Testing spatial segregation using a nearest-neighbor contingency table. Ecology 75 (7), 1940–1948.
Doherty, M.L., Chequer, A.D., Mass, T., Goodbody-Gringley, G., 2024. Phenotypic variability of Montastraea cavernosa and Porites astreoides along a depth gradient from shallow to mesophotic reefs in the Cayman Islands. Coral Reefs 43 (5), 1173–1187.
Domokos, G., Goriely, A., Horváth, Á.G., Regoős, K., 2024. Soft cells and the geometry of seashells. PNAS Nexus 3 (9), 311.
Dornelas, M., Madin, J.S., Baird, A.H., Connolly, S.R., 2017. Allometric growth in reef-building corals. Proc. R. Soc. B: Biol. Sci. 284 (1851), 20170053.
Fedorowski, J., 1980. Some aspects of coloniality in corals. Acta Palaeontol. Pol. 25 (3–4).
Foster, A.B., Johnson, K.G., Schultz, L.L., 1988. Allometric shape change and heterochrony in the freeliving coral Trachyphyllia bilobata (Duncan). Coral Reefs 7, 37–44.
Gateno, D., Rinkevich, B., 2003. Coral polyp budding is probably promoted by a canalized ratio of two morphometric fields. Mar. Biol. 142, 971–973.
Geyer, O.F., 1954. Die oberjurassische Korallenfauna von Württemberg. Palaeontogr. Abt. A 121–220.
Hiebert, L.S., Simpson, C., Tiozzo, S., 2021. Coloniality, clonality, and modularity in animals: The elephant in the room. J. Exp. Zoöl. B: Mol. Dev. Evol. 336 (3), 198–211.
Highsmith, R.C., 1982. Reproduction by fragmentation in corals.. Mar. Ecol. Prog. Ser. Oldendorf 7 (2), 207–226.
Houlbrèque, F., Ferrier-Pagès, C., 2009. Heterotrophy in tropical scleractinian corals. Biological Rev. 84 (1), 1–17.
Hughes, R., 1983. Evolutionary ecology of colonial reef-organisms, with particular reference to corals. Biol. J. Linnean Soc. 20 (1), 39–58.
Hughes, T.P., Baird, A.H., Bellwood, D.R., Card, M., Connolly, S.R., Folke, C., Grosberg, R., Hoegh-Guldberg, O., Jackson, J.B., Kleypas, J., et al., 2003. Climate change, human impacts, and the resilience of coral reefs. Science 301 (5635), 929–933.
Hughes, T.P., Barnes, M.L., Bellwood, D.R., Cinner, J.E., Cumming, G.S., Jackson, J.B., Kleypas, J., Van De Leemput, I.A., Lough, J.M., Morrison, T.H., et al., 2017. Coral reefs in the Anthropocene. Nature 546 (7656), 82–90.
Hughes, T.P., Jackson, J., 1985. Population dynamics and life histories of foliaceous corals. Ecol. Monograph. 55 (2), 141–166.
Jia, S., Shen, T., Cai, W., Zhang, J., Chen, S., 2025. Complete mitochondrial genome of platygyra daedalea and characteristics analysis of the mitochondrial genome in merulinidae. Genes 16 (3), 304.
Johanson, A.N., Flögel, S., Dullo, W.-C., Linke, P., Hasselbring, W., 2017. Modeling polyp activity of Paragorgia arborea using supervised learning. Ecol. Inform. 39, 109–118.
Jones, F.W., 1907. On the growth-forms and supposed species in corals. Proc. Zool. Soc. Lond. 77 (3), 518–556.
Jones, C.G., Lawton, J.H., Shachak, M., 1994. Organisms as ecosystem engineers. Ecosyst. Manag. 130–147.
Jung, J., Zoppe, S.F., Söte, T., Moretti, S., Duprey, N.N., Foreman, A.D., Wald, T., Vonhof, H., Haug, G.H., Sigman, D.M., et al., 2024. Coral photosymbiosis on mid-devonian reefs. Nature 1–7.
Kaandorp, J.A., Sloot, P.M., Merks, R.M., Bak, R.P., Vermeij, M.J., Maier, C., 2005. Morphogenesis of the branching reef coral Madracis mirabilis. Proc. R. Soc. B: Biol. Sci. 272 (1559), 127–133.
Kai, S., Sakai, K., 2008. Effect of colony size and age on resource allocation between growth and reproduction in the corals Goniastrea aspera and Favites chinensis. Mar. Ecol. Prog. Ser. 354, 133–139.
Kramer, N., Guan, J., Chen, S., Wangpraseurt, D., Loya, Y., 2022. Morpho-functional traits of the coral Stylophora pistillata enhance light capture for photosynthesis at mesophotic depths. Commun. Biol. 5 (1), 861.
Lartaud, F., Galli, G., Raza, A., Priori, C., Benedetti, M.C., Cau, A., Santangelo, G., Iannelli, M., Solidoro, C., Bramanti, L., et al., 2016. Growth patterns in long-lived coral species. Mar. Anim. For. 2, 595–626.
Lartaud, F., Pareige, S., de Rafelis, M., Feuillassier, L., Bideau, M., Peru, E., De la Vega, E., Nedoncelle, K., Romans, P., Le Bris, N., 2014. Temporal changes in the growth of two Mediterranean cold-water coral species, in situ and in aquaria. Deep. Sea Res. Part II: Top. Stud. Ocean. 99, 64–70.
Li, Y., Han, T., Bi, K., Liang, K., Chen, J., Lu, J., He, C., Lu, Z., 2020. The 3D reconstruction of Pocillopora colony sheds light on the growth pattern of this reef-building coral. Iscience 23 (6).
Li, Y., Liao, X., Wang, X., Li, Y., Zhao, H., Zhao, Y., Chen, J., He, C., Lu, Z., 2023. Polyp-canal reconstruction reveals evolution toward complexity in corals. Research 6, 0166.
Llabrés, E., Re, E., Pluma, N., Sintes, T., Duarte, C.M., 2024. A generalized numerical model for clonal growth in scleractinian coral colonies. Proc. R. Soc. B 291 (2030), 20241327.
Lovell, R.S., Collins, S., Martin, S.H., Pigot, A.L., Phillimore, A.B., 2023. Space-for-time substitutions in climate change ecology and evolution. Biol. Rev. 98 (6), 2243–2270.
Mackie, G., 1986. From aggregates to integrates: physiological aspects of modularity in colonial animals. Philos. Trans. R. Soc. Lond. B Biol. Sci. 313 (1159), 175–196.
Marfenin, N., 1997. Adaptation capabilities of marine modular organisms. In: Interactions and Adaptation Strategies of Marine Organisms: Proceedings of the 31st European Marine Biology Symposium, Held in St. Petersburg, Russia, 9–13 September 1996. Springer, pp. 153–158.
Matthai, G., 1926. VIII. Colony-formation in astrœid corals. Philos. Trans. R. Soc. Lond. Ser. B Contain. Pap. A Biol. Character 214 (411–420), 313–367.
Medellín-Maldonado, F., López-Pérez, A., Ruiz-Huerta, L., Carricart-Ganivet, J.P., 2022. Understanding corallite demography to comprehend potential bias in sclerochronology: Analysis of coral modular growth by micro-computed tomography. Limnol. Oceanogr. 67 (12), 2665–2676.
Merks, R.M., Hoekstra, A.G., Kaandorp, J.A., Sloot, P.M., 2004. Polyp oriented modelling of coral growth. J. Theoret. Biol. 228 (4), 559–576.
Oliver, W.A., 1968. Some aspects of colony development in corals. J. Paleontol. 42 (S2), 16–34.
O'Neill, R.V., 1986. A Hierarchical Concept of Ecosystems, No. 23. Princeton University Press.
Pandolfi, J.M., 1988. Heterochrony in colonial marine animals. In: Heterochrony in Evolution: A Multidisciplinary Approach. Springer, pp. 135–158.
Pandolfi, J.M., 1992. Successive isolation rather than evolutionary centres for the origination of Indo-Pacific reef corals. J. Biogeogr. 593–609.
Poty, E., 2010. Morphological limits to diversification of the rugose and tabulate corals. Palaeoworld 19 (3–4), 389–400.
Rachmilovitz, E.N., Shabbat, O., Yerushalmy, M., Rinkevich, B., 2022. Initiating a DNA barcoding reference library of stony corals from the Gulf of Eilat (Red Sea). J. Mar. Sci. Eng. 10 (12), 1917.
Rapuano, H., Shlesinger, T., Roth, L., Bronstein, O., Loya, Y., 2023. Coming of age: Annual onset of coral reproduction is determined by age rather than size. Iscience 26 (5).

Re, E., Schmidt-Roach, S., Llabres, E., Sintes, T., Duarte, C.M., 2024. Chapter clonal growth patterns in colonial anthozoan corals. In: Oceanography and Marine Biology. Taylor & Francis.
Riedl, R., 1978. Order in Living Organisms: A Systems Analysis of Evolution. John Wiley & Sons.
Rosen, B.R., 1986. Modular growth and form of corals: a matter of metamers? Philos. Trans. R. Soc. Lond. B Biol. Sci. 313 (1159), 115–142.
Rougvie, A., 2013. Heterochronic mutation. In: Brenner's Encyclopedia of Genetics: Second Edition. Elsevier Inc., pp. 442–445.
Sakai, K., 1998. Effect of colony size, polyp size, and budding mode on egg production in a colonial coral. Biol. Bull. 195 (3), 319–325.
Scrutton, C.T., 1998. The Palaeozoic corals, II: structure, variation and palaeoecology. Proc. Yorks. Geol. Soc. 52 (1), 1–57.
Shmuel, Y., Ziv, Y., Rinkevich, B., 2022. Strahler ordering analyses on branching coral canopies: Stylophora pistillata as a case study. J. Mar. Sci. Eng. 10 (1), 121.
Simpson, C., 2012. The evolutionary history of division of labour. Proc. R. Soc. B: Biol. Sci. 279 (1726), 116–121.
Simpson, C., 2021. An ecological driver for the macroevolution of morphological polymorphism within colonial invertebrates. J. Exp. Zoöl. Part B: Mol. Dev. Evol. 336 (3), 231–238.
Simpson, C., Herrera-Cubilla, A., Jackson, J.B., 2020. How colonial animals evolve. Sci. Adv. 6 (2), eaaw9530.
Simpson, C., Jackson, J.B., Herrera-Cubilla, A., 2017. Evolutionary determinants of morphological polymorphism in colonial animals. Amer. Nat. 190 (1), 17–28.
Smith, J.E., Brainard, R., Carter, A., Grillo, S., Edwards, C., Harris, J., Lewis, L., Obura, D., Rohwer, F., Sala, E., et al., 2016. Re-evaluating the health of coral reef communities: baselines and evidence for human impacts across the central Pacific. Proc. R. Soc. B: Biol. Sci. 283 (1822), 20151985.
Soong, K., Lang, J.C., 1992. Reproductive integration in reef corals. Biol. Bull. 183 (3), 418–431.
Stanley Jr., G.D., 2003. The evolution of modern corals and their early history. Earth-Sci. Rev. 60 (3–4), 195–225.
Stanley Jr., G., Van De Schootbrugge, B., 2009. The evolution of the coral–algal symbiosis. In: Coral Bleaching: Patterns, Processes, Causes and Consequences. Springer, pp. 7–19.
Stolarski, J., Kitahara, M.V., Miller, D.J., Cairns, S.D., Mazur, M., Meibom, A., 2011. The ancient evolutionary origins of Scleractinia revealed by azooxanthellate corals. BMC Evol. Biol. 11, 1–11.
Studivan, M.S., Milstein, G., Voss, J.D., 2019. Montastraea cavernosa corallite structure demonstrates distinct morphotypes across shallow and mesophotic depth zones in the Gulf of Mexico. PLoS One 14 (3), e0203732.
Todd, P., Sanderson, P., Chou, L., 2001. Morphological variation in the polyps of the scleractinian coral favia speciosa (Dana) around Singapore. Hydrobiologia 444, 227–235.
Tuomi, J., Vuorisalo, T., 1989. Hierarchical selection in modular organisms. Trends Ecol. Evolut. 4 (7), 209–213.
Veron, J., 1986. Corals of Australia and the Indo-Pacific. Angus & Robertson, North Ryde, N.S.W.
Veron, J., Stafford-Smith, M., Turak, E., DeVantier, L., 2016. Corals of the world. URL https://www.coralsoftheworld.org/page/structure-and-growth/. (Accessed 5 May 2025).
Wolfram, S., 1984. Cellular automata as models of complexity. Nature 311 (5985), 419–424.
Woodhead, A.J., Hicks, C.C., Norström, A.V., Williams, G.J., Graham, N.A., 2019. Coral reef ecosystem services in the Anthropocene. Funct. Ecol. 33 (6), 1023–1034.
Woodroffe, C.D., 2011. Subsidence hypothesis of reef development. Encycl. Mod. Coral Reefs 1062–1067.
Wu, Y., Kirillov, A., Massa, F., Lo, W.-Y., Girshick, R., 2019. Detectron2. https://github.com/facebookresearch/detectron2.